JOURNAL OF AGRICULTURAL AND FOOD CHEMISTRY
ARTICLE

J. Agric. Food Chem. 2010, 58, 12941–12949 12941
DOI:10.1021/jf103265x

Ursolic Acid Induces Allograft Inflammatory Factor-1 Expression via a Nitric Oxide-Related Mechanism and Increases Neovascularization

Ai-Wei Lee,[†] Ta-Liang Chen,[‡,§] Chun-Ming Shih,[#,⊗] Chun-Yao Huang,[#,⊗] Nai-Wen Tsao,[⊥] Nen-Chung Chang,[#,⊗] Yung-Hsiang Chen,*[,△] Tsorng-Harn Fong,*[,†] and Feng-Yen Lin*[,⊗,#]

[†]Graduate Institute of Medical Sciences and Department of Anatomy, School of Medicine, College of Medicine, Taipei Medical University, Taipei, Taiwan, [‡]Department of Anesthesiology, School of Medicine, College of Medicine, Taipei Medical University, Taipei, Taiwan, [§]Department of Anesthesiology, Taipei Medical University Hospital, Taipei, Taiwan, [#]Division of Cardiology, Department of Internal Medicine, Taipei Medical University Hospital, Taipei, Taiwan, [⊥]Division of Cardiovascular Surgery, Department of Surgery, Taipei Medical University Hospital, Taipei, Taiwan, [⊗]Department of Internal Medicine, School of Medicine, College of Medicine, Taipei Medical University, Taipei, Taiwan, and [△]Graduate Institute of Integrated Medicine, College of Chinese Medicine, China Medical University, Taichung, Taiwan

Ursolic acid (UA), a triterpenoid compound found in plants, is used in the human diet and in medicinal herbs and possesses a wide range of biological benefits including antioxidative, anti-inflammatory, and anticarcinogenic effects. Endothelial expression of allograft inflammatory factor-1 (AIF-1) mediates vasculogenesis, and nitric oxide (NO) produced by endothelial NO (eNOS) represents a mechanism of vascular protection. It is unclear whether UA affects the neovascularization mediated by AIF-1 and eNOS expression. This study investigated the effects and mechanisms of UA on angiogenesis in vivo in hind limb ischemic animal models and in vitro in human coronary artery endothelial cells (HCECs). This study explored the impact of UA on endothelial cell (EC) activities in vitro in HCECs, vascular neovasculogenesis in vivo in a mouse hind limb ischemia model, and the possible role of AIF-1 in vasculogenesis. The results demonstrate that UA enhances collateral blood flow recovery through induction of neovascularization in a hind limb ischemia mouse model. In vitro data showed that UA increases tube formation and migration capacities in human endothelial cells, and exposing HCECs to UA increased AIF-1 expression through a NO-related mechanism. Moreover, UA administration increased capillary density and eNOS and AIF-1 expression in ischemic muscle. These findings suggest that UA may be a potential therapeutic agent in the induction of neovascularization and provide a novel mechanistic insight into the potential effects of UA on ischemic vascular diseases.

KEYWORDS: Allograft inflammatory factor-1; Chinese herbal medicine; endothelial nitric oxide synthase; neovascularization; ursolic acid

INTRODUCTION

Ursolic acid (3β-hydroxyurs-12-en-28-oic acid) (UA) is a triterpenoid compound found in plants. UA is used in the human diet and in medicinal herbs (*1*, *2*) in the free acid form or as aglycones of triterpenoid saponins (*3*). It is well-known that UA possesses a wide range of biological benefits including antioxidative (*4*, *5*), anti-inflammatory (*5*), and anticarcinogenic (*6*) effects. Increasing evidence suggests that UA may inhibit free radical induced lipid peroxidation (*7*), increase the activity of endothelial nitric oxide synthase (eNOS), inhibit nicotinamide adenine dinucleotide phosphate oxidase 4 expression (*8*), enhance nonenzymatic antioxidative activities (*4*), and regulate high glucose induced apoptosis (*9*). Administration of UA demonstrated pleiotropic benefits, including inhibition of isoproterenol-induced myocardial ischemia, hyperglycemia-induced monocytic apoptosis (*9*), ethanol-mediated liver and heart damage (*10*, *11*), and D-galactose-induced neurotoxicity in the brain (*12*). Additionally, UA appears to have anti-inflammatory actions such as inhibition of arachidonate metabolism (*13*), attenuation of inducible NOS and cyclooxygenase-2 expression (*14*), and attenuation of prostaglandin E2 synthesis (*15*). Therefore, administration of UA may effectively prevent symptoms such as redness, edema, heat sensation, and pain. These findings suggest that the pharmacological action of UA may offer therapeutic strategies for the treatment of inflammatory and oxidative stress-related disorders.

Despite the anti-inflammatory and antioxidative actions of UA, its effects on the angiogenic ability of endothelial cells (ECs)

*Authors to whom correspondence should be addressed [phone +886-2-27361661, ext. 3013; e-mail (T.-H.F.)thfong@tmu.edu.tw, (Y.-H.C.) yhchen@mail.cmu.edu.tw, and (F.-Y.L.)g870905@tmu.edu.tw].

Published on Web 11/12/2010

were controversial in previous studies. Casimiro et al. demonstrated in vitro that UA can inhibit angiogenesis by inhibiting EC proliferation, migration, and differentiation, but simultaneously showed that UA may increase the expression of urokinase and matrix metalloproteinase-2 (MMP-2), which triggers angiogenesis (*16*). Furthermore, Kiran et al. reported that UA treatment increased the expression of E-selectin, intracellular adhesion molecule (ICAM), vascular endothelial growth factor (VEGF), and fibroblast growth factor 2 (FGF-2) in human umbilical vein endothelial cells (HUVECs) (*17*). Thus, an intensive study of the effects of UA on angiogenesis in vitro in human cells and in vivo in animal models is necessary.

In 1995, Utans et al. identified and characterized a novel macrophage factor, allograft inflammatory factor-1 (AIF-1), in the cytokine-rich milieu of cardiac allografts and showed that up-regulation of AIF-1 may accelerate chronic rejection-associated infiltration of INF-γ-stimulated macrophages (*18*). Furthermore, increasing evidence demonstrated that inhibition of AIF-1 may significantly reduce macrophage and vascular smooth muscle cell activation and signal transduction during atherogenesis (*19*−*22*). AIF-1 plays key roles in vascular smooth muscle cells and macrophages, which are involved in vascular inflammation. In contrast, the expression and roles of AIF-1 in vascular ECs were uncharacterized until 2009. In 2009, Tian et al. demonstrated that AIF-1 expression in ECs mediates vasculogenesis (*23*). Furthermore, Jia et al. revealed that AIF-1 overexpression promotes cell cycle transition, presumably by up-regulation of basic fibroblast growth factor (*24*, *25*). In this study, we therefore explored the impact of UA on EC activities in vitro, vascular neovasculogenesis in vivo, and the possible role of AIF-1 in vasculogenesis.

MATERIALS AND METHODS

Reagents. UA (≥98.5% purity) and other reagents were purchased from Sigma-Aldrich Co. (St. Louis, MO). UA was dissolved in ethanol as a 10 mM stock solution and stored at 4 °C.

Animals. All animals were treated according to protocols approved by the Institutional Animal Care Committee of the Taipei Medical University (Taipei, Taiwan). The experimental procedures and animal care conformed to the *Guide for the Care and Use of Laboratory Animals* published by the U.S. National Institutes of Health (NIH Publication 85-23, revised 1996). Male outbred ICR mice (6−8 weeks old) were purchased from the National Laboratory Animal Center in Taiwan. All mice were kept in microisolator cages on a 12 h day/night cycle and on a commercial mouse chow diet (Scientific Diet Services, Essex, U.K.) with water ad libitum.

Thirty mice were used, and the animals were divided into six groups. Group 1 was the nave control group; group 2 received a hind limb ischemia operation at the end of week 1 of the experiment; group 3 received a hind limb ischemia operation at the end of week 1 and intraperitoneal injections of UA [2 mg/kg of body weight (BW)] at the end of weeks 1, 2, and 3; group 4 received a hind limb ischemia operation at the end of week 1 and intraperitoneal injections of UA (5 mg/kg of BW) at the end of weeks 1, 2, and 3; group 5 received intraperitoneal injections of UA (5 mg/kg of BW) only at the end of weeks 1, 2, and 3; and group 6 received an incision but did not receive hind limb ischemia operation (sham control).

Mouse Hind Limb Ischemic Experiment. Six-week-old male ICR mice were kept on a commercial mouse chow diet. After 1 week of experimentation, unilateral hind limb ischemia was induced by excising the right femoral artery as previously described (*26*). Briefly, the animals were anesthetized by intraperitoneal injection of Xylocaine (2 mg/kg of BW) plus Zoletil (containing a dissociative anesthetic, Tiletamine/Zolazepam at a ratio of 1:1; 5 mg/kg of BW). The proximal and distal portions of the femoral artery were ligated. Hind limb blood perfusion was measured with a laser Doppler perfusion imager system (Moor Instruments Limited, Devon, U.K.) before and after the surgery and then followed weekly. The animals were sacrificed at the end of the fourth experimental week. To avoid the influence of ambient light and temperature, the results are expressed as the ratio of perfusion in the right (ischemic) versus left (nonischemic) limb.

Biochemical Measurements. Blood samples for biochemical measurements were collected from each animal before, and at 1, 2, 3, and 4 weeks after, the start of the experiment. Samples were collected from the mandibular artery into sodium citrate-containing tubes and separated by centrifugation. Serum blood urea nitrogen (BUN), creatinine, alanine aminotransferase (ALT), and aspartate aminotransferase (AST) were measured using the SPOTCHEM automatic dry chemistry system (SP-4410; Arkray, Japan).

Morphometry and Immunohistochemistry. The liver, kidney, and whole ischemic limbs were harvested. The adhering tissues and femora were carefully removed, and samples were immersion-fixed with 4% buffered paraformaldehyde, performed on serial 5 μm thick paraffin-embedded sections.

Hematoxylin/eosin staining was used for liver and kidney morphometry. Immunohistochemical staining was performed on mouse ischemia skeletal muscle by using goat anti-CD31 (Santa Cruz Biotechnologies, Santa Cruz, CA), rabbit anti-eNOS (Millipore, Bedford, MA), rabbit antiphospho-eNOS (Millipore), and goat anti-AIF-1 (Abcam, Cambridge, MA) antibodies.

Cell Culture. Human coronary artery endothelial cells (HCECs) were purchased from Cascade Biologics (Portland, OR) and were grown in endothelial cell growth medium (medium 200, Cascade Biologics) supplemented with 2% fetal bovine serum (FBS), 1 μg/mL hydrocortisone, 10 ng/mL human epidermal growth factor, 3 ng/mL human fibroblast growth factor, 10 μg/mL heparin, 100 U/mL penicillin, 100 pg/mL streptomycin, and 1.25 mg/mL Fungizone (Gibco, Grand Island, NY). HCECs were grown at 37 °C in a humidified 5% CO_2 atmosphere and were used at passages 3−8. The growth medium was changed every other day until confluence. The purity of HCEC cultures was verified by immunostaining with a monoclonal antibody directed against endothelial-specific human von Willebrand factor (vWF; R&D Systems, Minneapolis, MN).

Measurement of Cytotoxicity and Proliferation by MTT Assay. Cell cytotoxicity of UA was analyzed by the 3-(4,5-dimethylthiazol-2-yl)-2,5-diphenyltetrazolium bromide (MTT) assay. HCECs (2×10^4 cells) were grown in 96-well plates and incubated with various concentrations (1−50 μM) of UA for 24 h. Subsequently, MTT (0.5 μg/mL) was applied to cells for 4 h to allow the conversion of MTT into formazan crystals. After washing with phosphate-buffered saline (PBS), the cells were lysed with dimethyl sulfoxide (DMSO), and the absorbance was read at 530 nm by using a DIAS Microplate Reader (Dynex Technologies, Chantilly, VA).

Endothelial Cell Tube Formation Assay. The tube formation assay was performed on HCECs to assess vasculogenesis capacity, which is believed to be important for new vessel formation. The in vitro tube formation assay was performed using the Angiogenesis Assay Kit (Chemicon, Brea, CA) (*27*) according to the manufacturer's protocol. In brief, ECMatrix gel solution was thawed at 4 °C overnight, mixed with ECMatrix diluent buffer, and placed in a 96-well plate at 37 °C for 1 h to allow the matrix solution to solidify. HCECs were harvested as described above with trypsin/ethylenediaminetetraacetic acid (EDTA), 10^4 cells were placed on the matrix solution with M200 medium with UA, and the samples were incubated at 37 °C for 12 h. Tubule formation was inspected under an inverted light microscope. Four representative fields were taken, and the average of the total area of complete tubes formed by cells was compared by Image-Pro Plus computer software.

Cell Wound-Healing Assay. The migration ability of UA-treated HCECs cells was assayed in a monolayer denudation assay as described (*28*). HCECs were cultured in a 12-well plate. The confluent cells (2×10^5/well) were wounded by scraping with a 100 μL pipet tip, which denuded a strip of the monolayer that was 300 μm in diameter. The cultures were washed twice with PBS, the medium was supplemented with 5% FBS, and the rate of wound closure was observed after 24 h. The distance of the gap was measured under a 4× phase objective of a light microscope (Olympus IX71, USA), monitored with a CCD camera (Macro FIRE 2.3A), and captured with a videographic system (Picture Frame Application 2.3 software).

F-Actin Staining and Immunofluorescence Staining. HCECs seeded on the cover slide (1×10^5 cells) and fixed with 4% paraformaldehyde were permeabilized for 10 min with 0.1% Triton X-100 solution. Nonspecific antigens were blocked with 2% bovine serum albumin for 30 min, followed by staining with rhodamine-conjugated phalloidin or goat anti-AIF-1

Table 1. Plasma Biochemical Characteristics ($n = 5$) in Experimental Mice[a]

				UA administration			
					hind limb ischemia		
	weeks	control	sham control	5 mg/kg BW	0 mg/kg BW	2 mg/kg BW	5 mg/kg BW
BUN (mg/dL)	0	17 ± 2	19 ± 5	20 ± 4	18 ± 6	19 ± 8	21 ± 5
	2	15 ± 5	16 ± 3	19 ± 6	18 ± 6	21 ± 5	20 ± 7
	4	12 ± 4	15 ± 6	19 ± 4	19 ± 3	20 ± 5	18 ± 4
creatinine (mg/dL)	0	1.5 ± 0.5	1.3 ± 0.2	1.8 ± 0.2	1.6 ± 0.1	1.4 ± 0.2	1.4 ± 0.2
	2	1.2 ± 0.6	1.2 ± 0.2	1.5 ± 0.4	1.6 ± 0.1	1.6 ± 0.1	1.1 ± 0.1
	4	1.4 ± 0.4	1.6 ± 0.3	1.5 ± 0.1	1.7 ± 0.0	1.7 ± 0.1	1.9 ± 0.1
AST (IU/L)	0	30 ± 9	35 ± 4	47 ± 7	38 ± 12	36 ± 7	37 ± 4
	2	36 ± 6	386 ± 27*	45.82 ± 7.8	250 ± 17*	280 ± 31*	258 ± 15*
	4	31 ± 8	35 ± 6	38 ± 4	47 ± 7	40 ± 6	43 ± 6
ALT (IU/L)	0	38 ± 8	35 ± 8	38 ± 10	37 ± 7	36 ± 7	37 ± 10
	2	41 ± 9	57 ± 11	42 ± 12	46 ± 8	47 ± 16	38 ± 5
	4	34 ± 7	47 ± 6	58 ± 7	39 ± 10	42 ± 11	41 ± 8

[a] UA, ursolic acid; BUN, blood urea nitrogen; AST, aspartate aminotransferase; ALT, alanine aminotransferase. Values are mean ± SD. *, $p < 0.05$ compared with 0 week at the same group.

(Abcam) antibody and incubation with the secondary antibody conjugated to fluorescein isothiocyanate (FITC). Nuclei were identified using 2-(4-amidinophenyl)-6-indolecarbamidine dihydrochloride (DAPI). The slides were observed with confocal microscopy.

Western Blot Analysis. Cells were lysed with lysis buffer [0.5 M NaCl, 50 mM Tris, 1 mM EDTA, 0.05% SDS, 0.5% Triton X-100, and 1 mM phenylmethanesulfonyl fluoride (PMSF)] for 30 min at 4 °C, and cell lysates were centrifuged at 4000*g* for 30 min at 4 °C. Protein concentration in the supernatants was measured using a Bio-Rad protein determination kit (Bio-Rad, Hercules, CA). The supernatants were subjected to 10% SDS-PAGE and transferred for 1 h at room temperature to polyvinylidene difluoride (PVDF) membranes. The membranes were treated for 1 h at room temperature with PBS containing 0.05% Tween 20 and 2% skimmed milk and incubated separately for 1 h at room temperature with mouse anti-eNOS (Millipore) or goat anti-human AIF-1 antibodies (Abcam). After washing, the membranes were incubated for 1 h at room temperature with horseradish peroxidase-conjugated rabbit anti-goat or mouse IgG. Immunodetection was performed using a chemiluminescence reagent and exposure to Biomax MR Film (Kodak, Rochester, NY).

Statistical Analyses. Values are expressed as means ± SEM. Statistical evaluation was performed using Student's *t* test and one- or two-way ANOVA followed by Dunnett's test. A probability value of $p < 0.05$ was considered to be significant.

RESULTS AND DISCUSSION

UA Enhances Recovery of Capillary Density in ICR Mice. During the experimental period, weight gain and final weight did not differ significantly among the groups of animals (data not shown). As shown in **Table 1**, serum BUN, creatinine, and ALT levels were not significantly different between groups, although the AST level increased in the groups that received the hind limb ischemia operation at the end of week 2. To ensure that the dosage of UA used in the present animal study was harmless, morphometric analyses of kidney and liver were performed. Compared with the nave control group, intraperitoneal administration of UA at 5 mg/kg of BW three times over 4 weeks did not cause kidney injury, including glomerulonephritis, compression of capillaries, and narrowing of the Bowman space, in experimental mice (**Figure 1A**). The liver samples of UA-administered mice did not show feathery degeneration, micro- and macrocellular fatty changes, periportal fibrosis, or vascular congestion (**Figure 1B**). These results indicate that mice treated with UA at 5 mg/kg of BW demonstrated normal kidney and liver functions as well as histology.

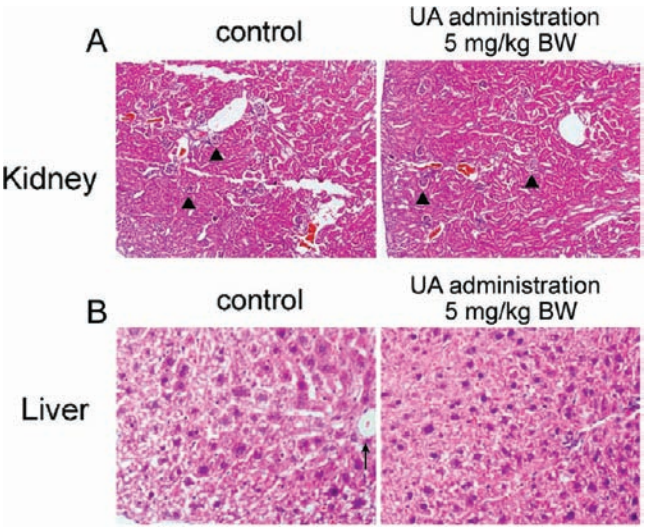

Figure 1. Control mice treated with UA demonstrated normal kidney and liver histology. (**A**) Control mouse kidney showing normal glomerulus (indicated by arrowheads). Following the control group, 5 mg/kg of BW UA administration 3 times over 4 weeks was harmless to kidney. (**B**) Control mouse liver showing central vein (indicated by black arrow) and hepatocytes arranged in the form of a cord. Liver of mouse administered UA also showed normal histology. Tissue samples were performed on serial 5 μm thick paraffin-embedded sections. Hematoxylin/eosin staining was used for morphometry (original magnification ×20).

To evaluate the angiogenic effect of UA, we induced tissue ischemia by unilateral hind limb ischemia surgery in wild-type male ICR mice ($n = 5$ for each group). The hind limb ischemic mice showed delayed blood flow recovery after ischemia surgery compared with control mice as determined by laser Doppler imaging, whereas intraperitoneal injection of UA at 2 and 5 mg/kg of BW significantly improved blood flow in hind limb ischemia-treated mice 2 weeks after ischemic surgery (the end of week 3) (**Figure 2A**,**B**). The blood flow of the limb was significantly changed in UA-treated and incision-receiving mice during the experimental period, but was not changed in control mice (**Figure 2B**). Three weeks following ischemic surgery (the end of experimental week 4), the ischemia/normal perfusion ratios were

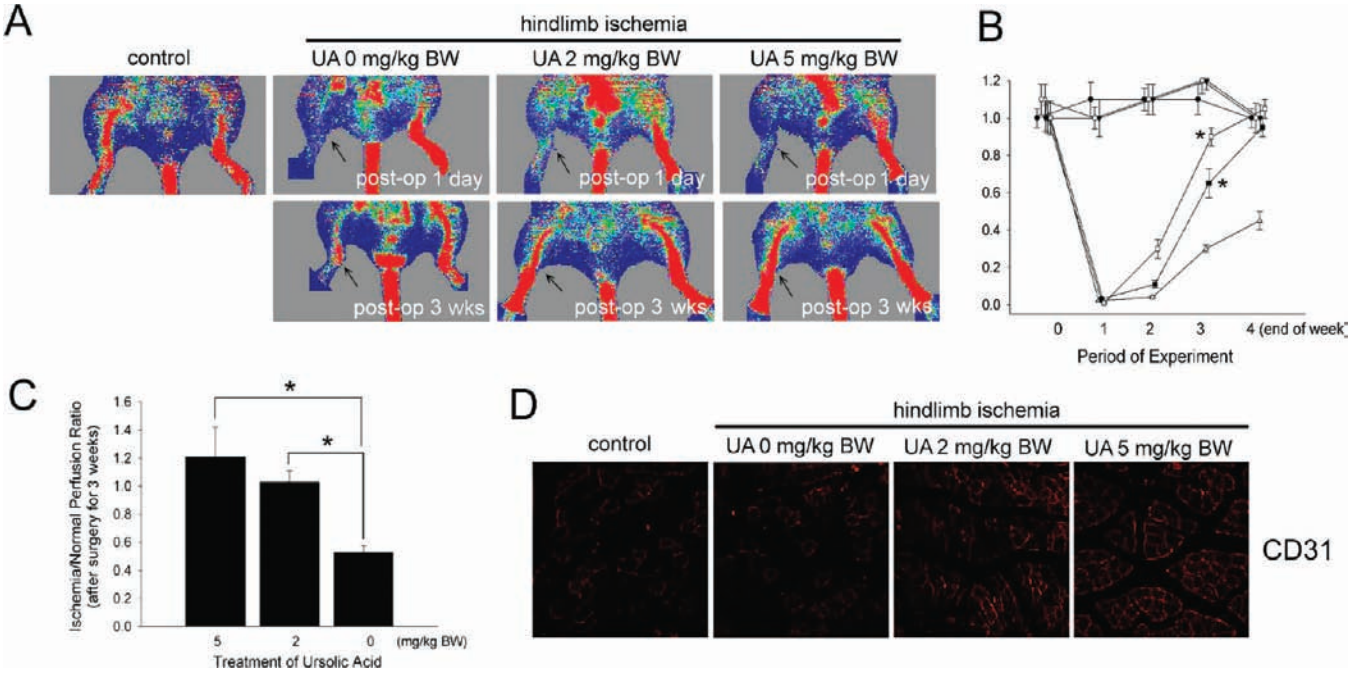

Figure 2. Effect of UA on blood flow recovery after hind limb ischemia in ICR mice. (**A**) Representative results of laser Doppler measurements before operation (control), 1 day and 3 weeks after hind limb ischemia surgery in 0, 2, or 5 mg/kg of BW UA administration mice. Color scale illustrates blood flow variations from minimal (dark blue) to maximal (red) values. Arrows indicate ischemic (right) limb after hind limb ischemia surgery. (**B**) Doppler perfusion ratios (ischemic/nonischemic hind limb) over time in the different groups. Administration of 2 (■) or 5 (□) mg/kg of BW UA provided the beneficial effect of blood flow recovery, compared with the nonadminstered group (□) after hind limb ischemia surgery for 2 weeks (the end of week 3 of the experiment). The blood flow of the limb did not significantly change in control (●), only UA-treated (○), and only incision-received mice (▼). Results are mean ± SEM (∗, $p < 0.05$ compared with non-UA-administered group (□). (**C**) After ischemic surgery for 3 weeks (the end of week 4 of the experiment), the ischemia/normal perfusion ratio in the UA-treated group was higher than that in the non-UA-treated group. Results are mean ± SEM (∗, $p < 0.05$ was considered to be significant). (**D**) Mice were sacrificed 3 weeks after surgery, and capillaries in the ischemic muscles were visualized by anti-CD31 immunostaining.

higher in the UA-treated group than in the non-UA-treated group (**Figure 2C**). Consistent with the measurements by laser Doppler imaging, anti-CD31 immunostaining revealed that UA administration at both 2 and 5 mg/kg of BW significantly increased the number of detectable capillaries in the ischemic muscle of treated mice (**Figure 2D**) compared to untreated ischemic mice. These results indicate that UA treatment may enhance the recovery of capillary density after hind limb ischemia in ICR mice.

We established the dose of UA on the basis of our pilot experiment, which was performed according to a previous animal study (*29*). The acute toxicity (LD_{50}) of UA on mice is > 637 mg/kg (intraperitoneal) and 8330 mg/kg (oral). The pharmacokinetic parameters of UA in rats after oral administration (80.32 mg/kg) are C_{max} = 294.8 ng/mL, t_{max} = 1.0 h, K_e = 0.16/h, and $t_{1/2}$ = 4.3 h (*30*). The pharmacokinetic data from Liao et al. suggest that the absorption of UA was rapid but its concentration in rat plasma was extremely low after oral administration. This implies either that UA has high binding activity in organs and low blood distribution or that UA is metabolized by the gut wall and liver but is poorly absorbed by the intestine (*30*).

UA Increases Proliferation, Tube Formation, and Migration of HCECs. The MTT assay was performed to analyze the cell viability and cytotoxicity of UA. Treatment of HCECs with 1 μM UA for 12 and 24 h or with 2.5 μM UA for 12 h did not result in cell viability changes or cell cytotoxicity (**Figure 3**). In contrast, > 5 μM UA may cause significantly reduced cell viability. Interestingly, HCECs treated with UA at 2.5 μM for 24 h and at 5 μM for 12 or 24 h showed significantly increased cell proliferation (125.4 ± 12.5, 120.6 ± 14.3, or 132.8 ± 6.5% of control, respectively). The results indicate that a moderate

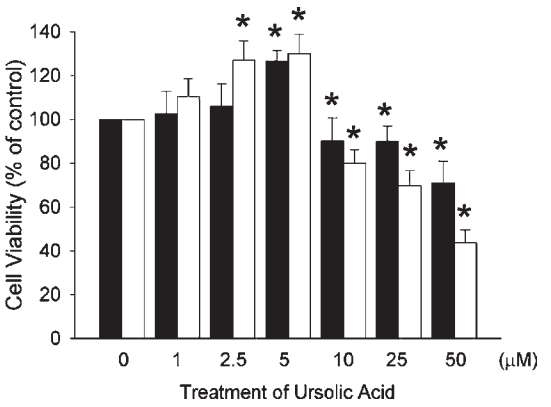

Figure 3. Effects of UA on cytotoxicity and proliferation were analyzed by the MTT assay: treatment of HCECs with 1−50 μM UA for 12 (■) or 24 (□) h. The MTT assay was performed and the absorbance was recorded using a microplate reader. Data are expressed as the mean ± SEM of three experiments performed in triplicate [∗, $p < 0.05$ compared with control (non-UA treated) at the same time point and considered to be significant].

concentration (2.5−5 μM) of UA increases eeHCEC proliferation, whereas a higher concentration induces cell cytotoxicity.

To explore the potential effects of UA on EC neovascularization, tube formation, and migration, assays were performed on HCECs. It has been shown that ECs successfully generate capillary network formation on Matrigel (*16*). After 24 h of culturing in 2.5 or 5 μM UA, the functional capacity for tube formation of HCECs on ECMatrix gel was significantly increased compared with the control group (200.1 ± 36.9 and 258.4 ± 28.4% of control, respectively) (**Figure 4A**,**B**). A previous study

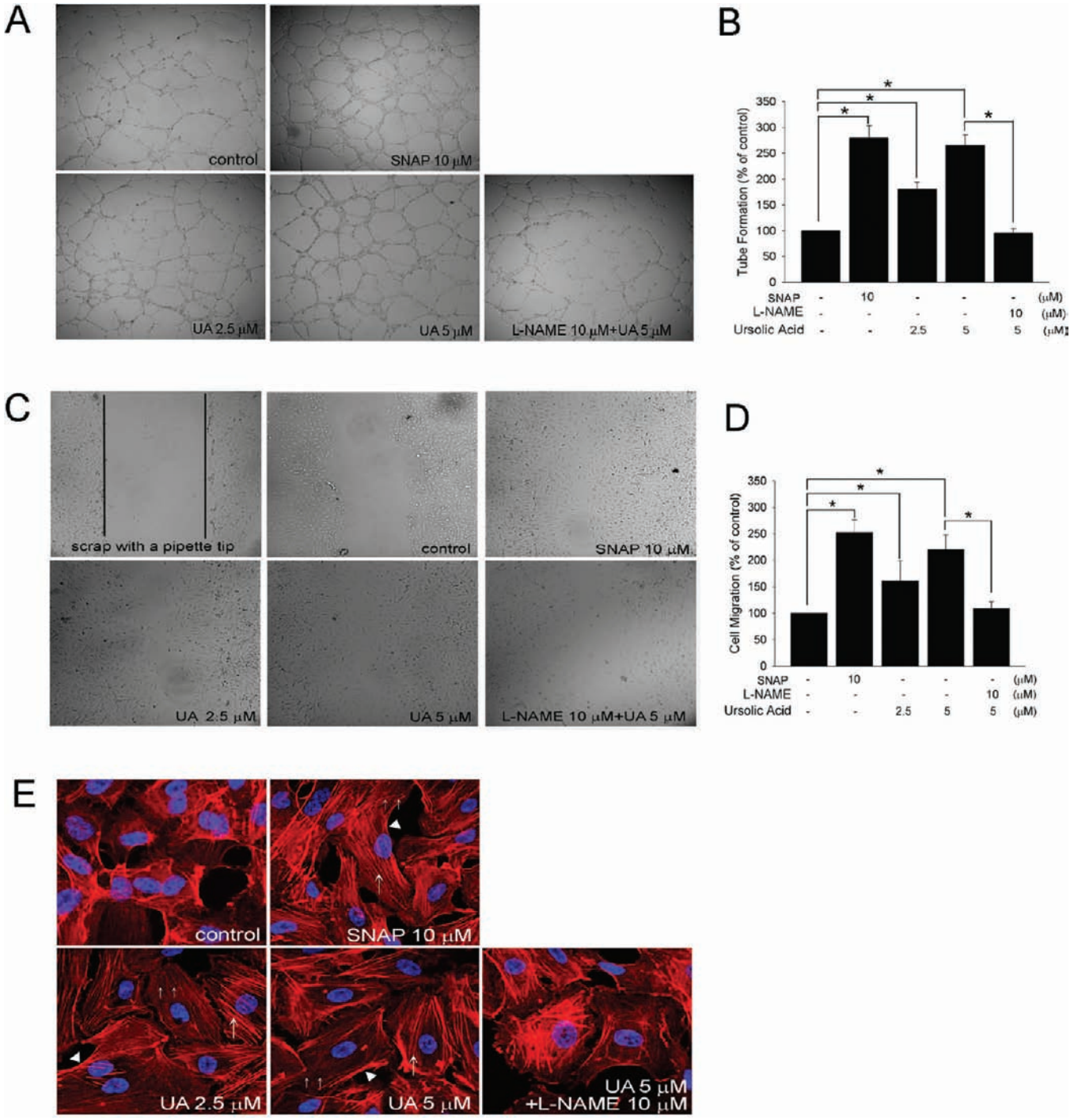

Figure 4. Effects of UA on the ability of tube formation and wound-healing in HCECs. (**A**) An in vitro angiogenesis assay for HCECs was used with ECMatrix gel. Representative photos for in vitro angiogenesis are shown. (**B**) The cells were stained with crystal violet, and the averages of the total area of complete tubes formed by cells were compared by computer software. Data are mean ± SEM; $n = 5$ (∗, $p < 0.05$ considered to be significant). (**C**) Wound-healing assay for evaluating the effect of UA on HCECs migration. The HCECs migrating to the denuded area were counted on the basis of the black baseline. The HCECs were cultured with 2.5 or 5 μM UA and 10 μM SNAP for 24 h or pretreated with 10 μM L-NAME for 2 h followed by 5 μM UA before wound scraping using a pipet tip. Photographs were taken after wound scraping for 18 h. (**D**) The cells that migrated into the denuded area were analyzed; the magnitude of HCECs migration was evaluated by counting the migrated cells in six random clones under high-power microscope fields (×100). Data are expressed as the mean ± SEM of three independent experiments and expressed as the percentage of control (∗, $p < 0.05$ was considered to be significant). (**E**) HCECs were treated as in (**A**). F-actin was stained with rhodamine−phalloidin, and the magnitude was evaluated using confocal microscope at 100× fields. The visible parallel stress fibers are indicated with a white arrow. The peripheral bands and cluster of F-actin are indicated with arrowheads. The disappeared individual stress fibers are indicated with a double arrow. DAPI was used to identify the nuclei of THP-1 cells.

demonstrated that eNOS regulates angiogenesis associated with oxidative stress in response to tissue ischemia (*31*). Incubation with a 10 μM concentration of the NO donor *S*-nitroso-*N*-acetylpenicillamine (SNAP) for 24 h significantly increased tube formation function in HCECs, whereas preincubation with the NOS inhibitor L-N^{ω}-nitro-L-arginine methyl ester (L-NAME) for 2 h decreased the effect of UA on tube formation. Treatment of cells with 2.5 μM UA, 5 μM UA, or 10 μM SNAP for 24 h induced

their wound-healing/migratory abilities in a dose-dependent manner (200.1 ± 36.9, 258.4 ± 28.4, or 290.9 ± 24.1% of control, respectively). After treatment with L-NAME (10 μM) for 2 h, the migratory abilities of HCECs were significantly reduced (109.3 ± 12.4% of control) compared with the UA-treated group (**Figure 4C**,**D**).

The cytoskeleton is a key component that allows cells to maintain proliferation and migration (*32*, *33*). HCECs were treated with UA for 24 h and were fixed and stained for F-actin using phalloidin−rhodamine to study the effect of UA on cytoskeleton organization. **Figure 4E** shows that nave HCECs presented with a cobblestone pattern, and the distribution of F-actin was in a crisscross pattern. However, treatment with either 2.5−5 μM UA or 10 μM SNAP resulted in the presence of stress fibers that were visible in a parallel pattern (white arrow) and that crossed the cell from one side to the other. Additionally, HCECs displayed peripheral bands and clusters of F-actin (arrowhead) in the margin as well as the partial disappearance of individual stress fibers (double arrow), indicating the redistribution of F-actin. Pretreatment with L-NAME may reverse the effect of UA on F-actin reorganization. These results suggest that UA might effectively stimulate tube formation and migration of HCECs, which mediate NOS activity and cytoskeleton reorganization.

UA is the major component of some traditional medicinale herbs and is known to possess a wide range of biological functions such as antioxidative, anti-inflammatory, and anticancer activities. In contrast to these beneficial properties, some laboratory studies have recently revealed that the effects of UA on normal cells and tissues are occasionally pro-inflammatory (*34*). On the other hand, little information is available regarding the angiogenic effect of UA. Sohn et al. first examined the antiangiogenic activity of UA by using the chick embryo chorioallantoic membrane assay. This group also tested for an inhibitory effect on the proliferation of bovine aortic endothelial cells. On the basis of their results, they speculated that the inhibitory effects of UA on bovine aortic endothelial cell proliferation might be important for antiangiogenesis (*35*). Cárdenas et al. studied the effects of UA on different key steps of angiogenesis and found that UA can inhibit key steps of angiogenesis in vitro, including endothelial cell proliferation, migration, and differentiation. At the same time, UA appeared to stimulate other key steps of angiogenesis such as extracellular matrix degradation by MMP-2 and urokinase (*17*). More recently, UA was found to inhibit tumor-associated capillary formation in mice induced by highly metastatic melanoma cells. Nontoxic concentrations of UA reduced vessel growth from the rat aortic ring and inhibited proliferation, migration, and invasion of ECs. Gelatin zymographic analysis showed that UA had an inhibitory effect on the protein expression of matrix metalloproteinases MMP-2 and MMP-9 (*36*). The above observations demonstrate the antiangiogenic activity of UA. In contrast, Kiran et al. reported the up-regulation of angiogenic modulators in ECs treated with UA; however, low concentrations of UA (< 10 μM) had no effect on these modulators. The cells were maintained in culture in serum-free, unstimulated conditions. The changes in the angiogenic modulators correlated with the ability of UA to influence angiogenesis. Treatment with UA at higher concentrations promoted angiogenesis, which was evidenced by tube formation of HUVECs and a greater extent of endothelial sprouting in rat aortic rings, but no such effects were observed at low concentrations. However, UA treatment of HUVECs and aortic rings that were stimulated by maintenance in medium supplemented with serum inhibited the angiogenic phenotype (*17*). Our present study showed that UA enhances collateral blood flow recovery by inducing neovascularization. Low concentrations (≤5 μM) of UA increase the tube formation and migration capacities in human ECs. Interestingly, the in vitro results indicate that low concentrations of UA increase HCEC proliferation, whereas higher concentrations (≥10 μM) induce cell cytotoxicity in ECs. Similarly, statins have proangiogenic effects at low therapeutic concentrations but angiostatic effects at high concentrations, suggesting that statins have a biphasic dose-dependent effect on angiogenesis (*37*−*39*). Thus, UA might be considered a double-edged sword, with both positive and negative effects on angiogenesis. Further evaluation of the effects of UA on the biological status of target cells or tissues is necessary.

UA Increases AIF-1 Expression through Phosphorylation of eNOS in Vitro and Increases Capillary Density, eNOS, and AIF-1 Expression in Vivo. AIF-1 expression regulates endothelial cell signal transduction, which mediates proliferation and vasculogenesis (*23*, *25*). Treating HCECs with 1−5 μM UA for 12−24 h may result in increased intracellular AIF-1 expression (**Figure 5A**). Additionally, previous studies suggest that vascular eNOS-derived NO is a main factor in the maintenance of vascular physiology (*33*, *40*). We therefore investigated the effects of UA on the NO system in HCECs. After 24 h of incubation, eNOS phosphorylation at Ser^{1177} as determined by immunoblotting was significantly increased in HCECs cultured in 1−5 μM UA-containing medium compared to control conditions (**Figure 5B**). On the other hand, phosphorylation of eNOS occurred in a time-dependent manner in 5 μM UA-treated HCECs (**Figure 5C**). To explore the involvement of vascular NO in AIF-1 expression, we treated HCECs with a 10 μM concentration of the NO donor SNAP for 24 h. The results indicate that intracellular AIF-1 expression is regulated by the NO level. In contrast, co-incubation with a 10 μM concentration of the NOS inhibitor L-NAME significantly attenuated the UA-induced increase in AIF-1 expression in HCECs (**Figure 5D**). Consistent with Western blot analysis, confocal microscopy revealed that UA and SNAP incubation for 24 h resulted in a marked accumulation of AIF-1, whereas treatment with 10 μM L-NAME appeared to reverse this phenomenon (**Figure 5E**). These data indicate that UA may up-regulate AIF-1 expression by modulating NO-related mechanisms.

To extend our in vitro observations, we performed measurements of eNOS and AIF-1 expression on histological sections harvested from the ischemic hind limbs of mice. The number of detectable capillaries (white arrow) and level of eNOS expression (arrowhead) from limb ischemia were significantly increased in mice treated with UA at 2 and 5 mg/kg of BW compared to controls (**Figure 6A**). These images indeed show that eNOS was increased in the region of capillaries. We next examined whether UA increased AIF-1 expression in the ischemic hind limb muscle of mice. UA administration appeared to increase the expression of AIF-1 in ischemic muscle compared to controls (**Figure 6B**). These results indicate that UA treatment after hind limb ischemic surgery, especially at a concentration of 5 mg/kg of BW, may increase eNOS and AIF-1 expression in the muscle capillaries.

AIF-1 has been identified in chronic rejection of rat cardiac allografts as well as tissue inflammation in various autoimmune diseases. Kimura et al. first suggested that AIF-1 is closely associated with the pathogenesis of rheumatoid arthritis, which is characterized by massive synovial proliferation, angiogenesis, and subintimal infiltration of inflammatory cells (*41*). In addition, EC migration and proliferation have an important role in numerous physiological responses such as angiogenesis (*23*). AIF-1 protein expression has been detected in human arteries with coronary artery vasculopathy and in neointimal cells in animal models of various types of arterial injuries (*22*, *42*). AIF-1 is expressed in ECs of inflamed arteries and can be induced by soluble stimuli in cultured ECs. Inducible AIF-1 expression in ECs suggests an important role for this protein in EC activation, and abrogation

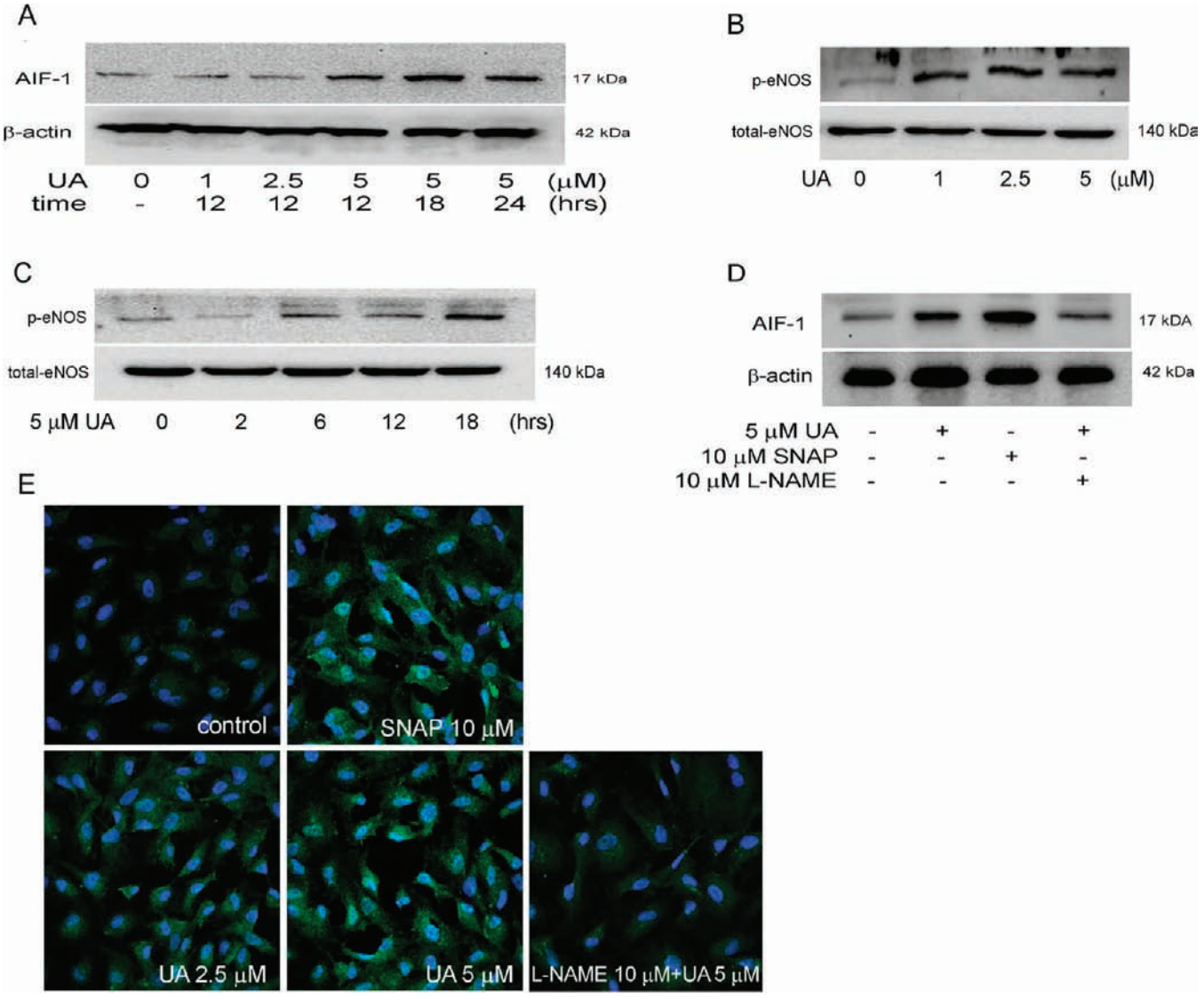

Figure 5. UA increased AIF-1 expression mediating by phosphorylation of eNOS in HCECs. (**A**) HCECs were treated for 12−24 h with 1−5 μM UA, and the AIF-1 expression was analyzed by Western blot analysis. (**B**) HCECs were treated for 18 h with 1−5 μM UA, and the eNOS activation (phosphorylation) was analyzed by Western blot analysis. (**C**) HCECs were treated for 2−18 h with 5 μM UA, and the eNOS activation was analyzed by Western blot analysis. (**D**) HCECs were treated for 24 h with 5 μM UA and 10 μM SNAP or pretreated with 10 μM L-NAME for 2 h prior to stimulation with UA for 24 h. AIF-1 production was analyzed by Western blot analysis. β-actin and total eNOS protein were used as loading controls. (**E**) HCECs were treated as in (**D**). Intracellular AIF-1 production was analyzed by immunofluorescence, and the magnitude was evaluated using confocal microscope at 40× fields. DAPI was used to identify the nuclei of THP-1 cells.

of AIF-1 expression significantly inhibited EC proliferation and migration (*23*). More recently, Jia et al. showed that stable introduction of AIF-1 into HUVECs in vitro resulted in enhanced proliferation and migration of ECs and promoted the G_0/G_1- to S-phase transition (*24*). Taken together, these findings suggest that AIF-1 stimulates EC activation and angiogenesis and consequently affects the progression of neovascularization in ischemia.

NO produced by eNOS represents a mechanism of vascular protection. NO bioavailability is decreased in atherosclerosis due to increased NO inactivation by reactive oxygen species and reduced NO synthesis. Various types of vascular pathophysiologies are associated with oxidative stress that inactivate NO. In addition, oxidative stress is likely the main cause for oxidation of the essential NOS cofactor tetrahydrobiopterin (*43*). Aguirre-Crespo et al. demonstrated that UA-mediated vascular relaxation is endothelium dependent, probably due to NO release (*44*). Recently, Steinkamp-Fenske et al. found that UA up-regulates eNOS and also reduces NADPH oxidase expression in human ECs through protein kinase C-independent mechanisms (*8*). Additionally, UA significantly increased eNOS expression in HUVECs and enhanced bioactive NO production. Interestingly, UA has also been found to reduce the expression of the NADPH oxidase subunit Nox4 and to suppress the production of reactive oxygen species in human endothelial cells (*8*). Our paper further shows that UA induces AIF-1 expression via a NO-related mechanism and increases neovascularization. To the best of our knowledge, this is the first study showing that UA increases AIF-1 expression, mediating by phosphorylation of eNOS in HCECs. On the other hand, because NO is generated by distinct isoforms of NOS [eNOS, neuronal (nNOS), and inducible (iNOS)], the role of iNOS (*45*) should also be studied in vascular protection, and the possible role of iNOS in UA-induced vasculogenesis should be further investigated.

In conclusion, our results demonstrate that UA enhances the recovery of capillary density through induction of neovascularization in a hind limb ischemia mouse model. UA increases tube

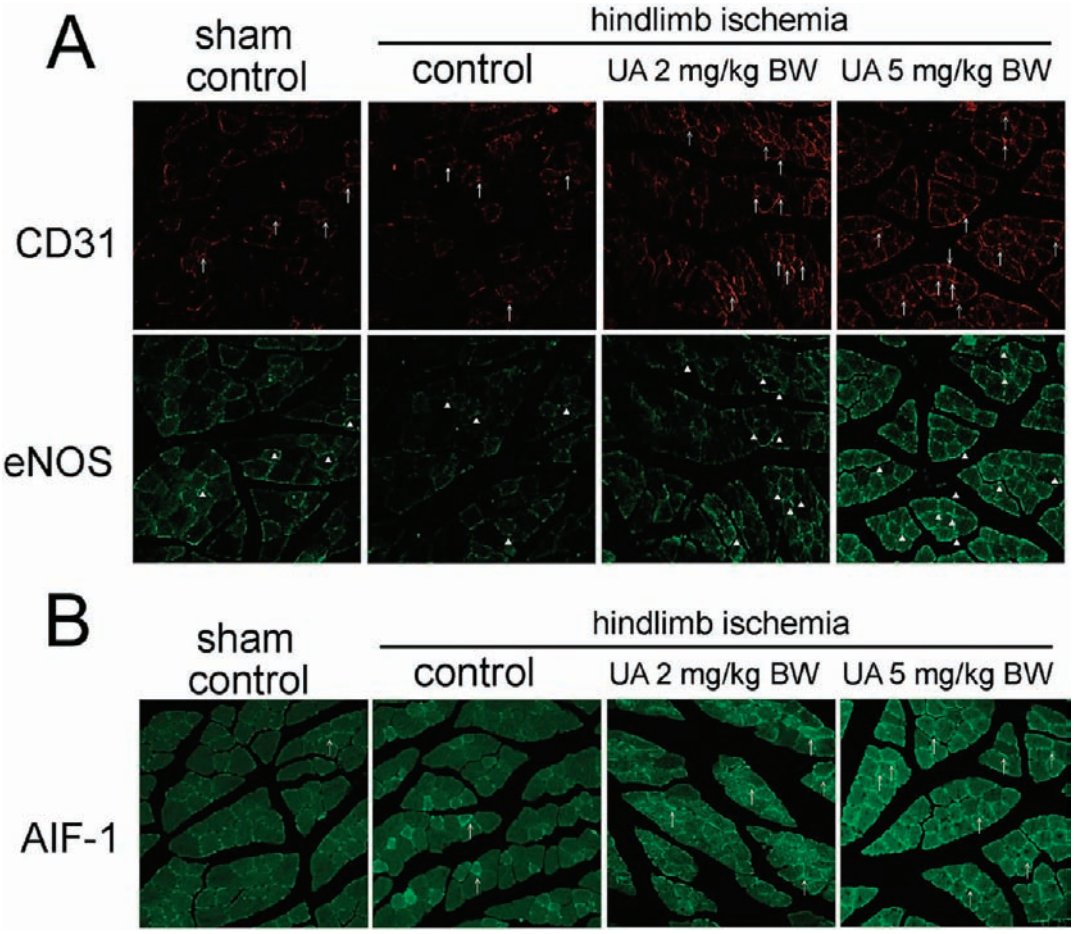

Figure 6. eNOS expression combined with capillary density and AIF-1 expression in ischemic hind limb tissue evaluated by immunohistochemistry and confocal microscopy at 40× fields. (**A**) Immunostaining of ischemic hind limb muscle with anti-CD31 conjugated Alex 633 (red) and anti-eNOS conjugated Alex 488 (green) antibodies. The arrows indicate the endothelium, and the arrowhead indicates the eNOS in the hind limb muscle. (**B**) Immunostaining of ischemic hind limb muscle with anti-AIF-1 conjugated Alex 488 (green) antibody. The arrows indicate the AIF-1 in the hind limb muscle.

formation and migration capacities in human ECs, and exposing HCECs to UA resulted in increased AIF-1 expression through a NO-related mechanism. Moreover, UA administration increased capillary density and eNOS and AIF-1 expression in ischemic muscle.

In the present study, we demonstrated for the first time that the triterpenoid compound UA enhances collateral blood flow recovery through induction of neovascularization in a hind limb ischemia mouse model. The in vitro data show that UA increases tube formation and migration capacities in human ECs and that exposing HCECs to UA results in increased AIF-1 expression through a NO-related mechanism. Moreover, UA administration increases capillary density and eNOS and AIF-1 expression in ischemic muscle. These findings suggest that UA may act as a therapeutic agent in the induction of neovascularization and provide a novel mechanistic insight into the potential effects of UA on ischemic vascular diseases. Further investigation of the regulation underlying UA-induced AIF-1 and the NO signaling pathway may contribute to the development of a new clinical strategy for ischemic vascular diseases.

ACKNOWLEDGMENT

We thank Tze-Liang Yang, Min-Yu Lo, and Ke Yea-Wen for technical assistance.

LITERATURE CITED

(1) Li, Y.; Kang, Z.; Li, S.; Kong, T.; Liu, X.; Sun, C. Ursolic acid stimulates lipolysis in primary-cultured rat adipocytes. *Mol. Nutr. Food Res.* **2010**.

(2) Yeh, C. T.; Wu, C. H.; Yen, G. C. Ursolic acid, a naturally occurring triterpenoid, suppresses migration and invasion of human breast cancer cells by modulating c-Jun N-terminal kinase, Akt and mammalian target of rapamycin signaling. *Mol. Nutr. Food Res.* **2010**.

(3) Furtado, R. A.; Rodrigues, E. P.; Araujo, F. R.; Oliveira, W. L.; Furtado, M. A.; Castro, M. B.; Cunha, W. R.; Tavares, D. C. Ursolic acid and oleanolic acid suppress preneoplastic lesions induced by 1,2-dimethylhydrazine in rat colon. *Toxicol. Pathol.* **2008**, *36*, 576−580.

(4) Yin, M. C.; Chan, K. C. Nonenzymatic antioxidative and antiglycative effects of oleanolic acid and ursolic acid. *J. Agric. Food Chem.* **2007**, *55*, 7177−7181.

(5) Tsai, S. J.; Yin, M. C. Antioxidative and anti-inflammatory protection of oleanolic acid and ursolic acid in PC12 cells. *J. Food Sci.* **2008**, *73*, H174−H178.

(6) Yan, S. L.; Huang, C. Y.; Wu, S. T.; Yin, M. C. Oleanolic acid and ursolic acid induce apoptosis in four human liver cancer cell lines. *Toxicol. In Vitro* **2010**, *24*, 842−848.

(7) Balanehru, S.; Nagarajan, B. Protective effect of oleanolic acid and ursolic acid against lipid peroxidation. *Biochem. Int.* **1991**, *24*, 981−990.

(8) Steinkamp-Fenske, K.; Bollinger, L.; Voller, N.; Xu, H.; Yao, Y.; Bauer, R.; Forstermann, U.; Li, H. Ursolic acid from the Chinese herb danshen (*Salvia miltiorrhiza* L.) upregulates eNOS and downregulates Nox4 expression in human endothelial cells. *Atherosclerosis* **2007**, *195*, e104−e111.

(9) Oh, C. J.; Kil, I. S.; Park, C. I.; Yang, C. H.; Park, J. W. Ursolic acid regulates high glucose-induced apoptosis. *Free Radical Res.* **2007**, *41*, 638−644.

(10) Saravanan, R.; Viswanathan, P.; Pugalendi, K. V. Protective effect of ursolic acid on ethanol-mediated experimental liver damage in rats. *Life Sci*. **2006**, *78*, 713−718.
(11) Saravanan, R.; Pugalendi, V. Impact of ursolic acid on chronic ethanol-induced oxidative stress in the rat heart. *Pharmacol. Rep*. **2006**, *58*, 41−47.
(12) Lu, J.; Zheng, Y. L.; Wu, D. M.; Luo, L.; Sun, D. X.; Shan, Q. Ursolic acid ameliorates cognition deficits and attenuates oxidative damage in the brain of senescent mice induced by D-galactose. *Biochem. Pharmacol*. **2007**, *74*, 1078−1090.
(13) Najid, A.; Simon, A.; Cook, J.; Chable-Rabinovitch, H.; Delage, C.; Chulia, A. J.; Rigaud, M. Characterization of ursolic acid as a lipoxygenase and cyclooxygenase inhibitor using macrophages, platelets and differentiated HL60 leukemic cells. *FEBS Lett*. **1992**, *299*, 213−217.
(14) Suh, N.; Honda, T.; Finlay, H. J.; Barchowsky, A.; Williams, C.; Benoit, N. E.; Xie, Q. W.; Nathan, C.; Gribble, G. W.; Sporn, M. B. Novel triterpenoids suppress inducible nitric oxide synthase (iNOS) and inducible cyclooxygenase (COX-2) in mouse macrophages. *Cancer Res*. **1998**, *58*, 717−723.
(15) Subbaramaiah, K.; Michaluart, P.; Sporn, M. B.; Dannenberg, A. J. Ursolic acid inhibits cyclooxygenase-2 transcription in human mammary epithelial cells. *Cancer Res*. **2000**, *60*, 2399−2404.
(16) Cardenas, C.; Quesada, A. R.; Medina, M. A. Effects of ursolic acid on different steps of the angiogenic process. *Biochem. Biophys. Res. Commun*. **2004**, *320*, 402−408.
(17) Kiran, M. S.; Viji, R. I.; Sameer Kumar, V. B.; Sudhakaran, P. R. Modulation of angiogenic factors by ursolic acid. *Biochem. Biophys. Res. Commun*. **2008**, *371*, 556−560.
(18) Utans, U.; Arceci, R. J.; Yamashita, Y.; Russell, M. E. Cloning and characterization of allograft inflammatory factor-1: a novel macrophage factor identified in rat cardiac allografts with chronic rejection. *J. Clin. Invest*. **1995**, *95*, 2954−2962.
(19) Tian, Y.; Kelemen, S. E.; Autieri, M. V. Inhibition of AIF-1 expression by constitutive siRNA expression reduces macrophage migration, proliferation, and signal transduction initiated by atherogenic stimuli. *Am. J. Physiol*. **2006**, *290*, C1083−C1091.
(20) Sommerville, L. J.; Kelemen, S. E.; Autieri, M. V. Increased smooth muscle cell activation and neointima formation in response to injury in AIF-1 transgenic mice. *Arteriosclerosis, Thrombosis, Vasc. Biol*. **2008**, *28*, 47−53.
(21) Sommerville, L. J.; Xing, C.; Kelemen, S. E.; Eguchi, S.; Autieri, M. V. Inhibition of allograft inflammatory factor-1 expression reduces development of neointimal hyperplasia and p38 kinase activity. *Cardiovasc. Res*. **2009**, *81*, 206−215.
(22) Autieri, M. V.; Carbone, C.; Mu, A. Expression of allograft inflammatory factor-1 is a marker of activated human vascular smooth muscle cells and arterial injury. *Arteriosclerosis, Thrombosis, Vasc. Biol*. **2000**, *20*, 1737−1744.
(23) Tian, Y.; Jain, S.; Kelemen, S. E.; Autieri, M. V. AIF-1 expression regulates endothelial cell activation, signal transduction, and vasculogenesis. *Am. J. Physiol*. **2009**, *296*, C256−C266.
(24) Jia, J.; Cai, Y.; Wang, R.; Fu, K.; Zhao, Y. F. Overexpression of allograft inflammatory factor-1 promotes the proliferation and migration of human endothelial cells (HUV-EC-C) probably by up-regulation of basic fibroblast growth factor. *Pediatr. Res*. **2010**, *67*, 29−34.
(25) Jia, J.; Cai, Y.; Wang, R.; Fu, K.; Zhao, Y. F. Overexpression of allograft inflammatory factor-1 promotes the proliferation and migration of human endothelial cells (HUV-EC-C) probably by up-regulation of basic fibroblast growth factor. *Pediatr. Res. 67*, 29−34.
(26) Huang, P. H.; Sata, M.; Nishimatsu, H.; Sumi, M.; Hirata, Y.; Nagai, R. Pioglitazone ameliorates endothelial dysfunction and restores ischemia-induced angiogenesis in diabetic mice. *Biomed. Pharmacother*. **2008**, *62*, 46−52.
(27) Chen, J. Z.; Zhu, J. H.; Wang, X. X.; Zhu, J. H.; Xie, X. D.; Sun, J.; Shang, Y. P.; Guo, X. G.; Dai, H. M.; Hu, S. J. Effects of homocysteine on number and activity of endothelial progenitor cells from peripheral blood. *J. Mol. Cell. Cardiol*. **2004**, *36*, 233−239.
(28) Tang, S.; Morgan, K. G.; Parker, C.; Ware, J. A. Requirement for protein kinase C theta for cell cycle progression and formation of actin stress fibers and filopodia in vascular endothelial cells. *J. Biol. Chem*. **1997**, *272*, 28704−28711.
(29) Pozo, M.; Castilla, V.; Gutierrez, C.; de Nicolas, R.; Egido, J.; Gonzalez-Cabrero, J. Ursolic acid inhibits neointima formation in the rat carotid artery injury model. *Atherosclerosis* **2006**, *184*, 53−62.
(30) Liao, Q.; Yang, W.; Jia, Y.; Chen, X.; Gao, Q.; Bi, K. LC-MS determination and pharmacokinetic studies of ursolic acid in rat plasma after administration of the traditional chinese medicinal preparation Lu-Ying extract. *Yakugaku Zasshi* **2005**, *125*, 509−515.
(31) Gigante, B.; Morlino, G.; Gentile, M. T.; Persico, M. G.; De Falco, S. Plgf−/−eNos−/− mice show defective angiogenesis associated with increased oxidative stress in response to tissue ischemia. *FASEB J*. **2006**, *20*, 970−972.
(32) Hall, A. Rho GTPases and the actin cytoskeleton. *Science* 1998, 279, 509−514.
(33) Su, Y.; Edwards-Bennett, S.; Bubb, M. R.; Block, E. R. Regulation of endothelial nitric oxide synthase by the actin cytoskeleton. *Am. J. Physiol*. **2003**, *284*, C1542−1549.
(34) Ikeda, Y.; Murakami, A.; Ohigashi, H. Ursolic acid: an anti- and pro-inflammatory triterpenoid. *Mol. Nutr. Food Res*. **2008**, *52*, 26−42.
(35) Sohn, K. H.; Lee, H. Y.; Chung, H. Y.; Young, H. S.; Yi, S. Y.; Kim, K. W. Anti-angiogenic activity of triterpene acids. *Cancer Lett*. **1995**, *94*, 213−218.
(36) Kanjoormana, M.; Kuttan, G. Antiangiogenic activity of ursolic acid. *Integr. Cancer Ther*. **2010**, *9*, 224−235.
(37) Weis, M.; Heeschen, C.; Glassford, A. J.; Cooke, J. P. Statins have biphasic effects on angiogenesis. *Circulation* **2002**, *105*, 739−745.
(38) Elewa, H. F.; El-Remessy, A. B.; Somanath, P. R.; Fagan, S. C. Diverse effects of statins on angiogenesis: new therapeutic avenues. *Pharmacotherapy* **2010**, *30*, 169−176.
(39) Sata, M. Biphasic effects of statins on angiogenesis. *Circulation* **2002**, *106*, e47; author reply, e47.
(40) Searles, C. D.; Ide, L.; Davis, M. E.; Cai, H.; Weber, M. Actin cytoskeleton organization and posttranscriptional regulation of endothelial nitric oxide synthase during cell growth. *Circ. Res*. **2004**, *95*, 488−495.
(41) Kimura, M.; Kawahito, Y.; Obayashi, H.; Ohta, M.; Hara, H.; Adachi, T.; Tokunaga, D.; Hojo, T.; Hamaguchi, M.; Omoto, A.; Ishino, H.; Wada, M.; Kohno, M.; Tsubouchi, Y.; Yoshikawa, T. A critical role for allograft inflammatory factor-1 in the pathogenesis of rheumatoid arthritis. *J. Immunol*. **2007**, *178*, 3316−3322.
(42) Autieri, M. V.; Kelemen, S.; Thomas, B. A.; Feller, E. D.; Goldman, B. I.; Eisen, H. J. Allograft inflammatory factor-1 expression correlates with cardiac rejection and development of cardiac allograft vasculopathy. *Circulation* **2002**, *106*, 2218−2223.
(43) Li, H.; Forstermann, U. Prevention of atherosclerosis by interference with the vascular nitric oxide system. *Curr. Pharm. Des*. **2009**, *15*, 3133−3145.
(44) Aguirre-Crespo, F.; Vergara-Galicia, J.; Villalobos-Molina, R.; Javier Lopez-Guerrero, J.; Navarrete-Vazquez, G.; Estrada-Soto, S. Ursolic acid mediates the vasorelaxant activity of *Lepechinia caulescens* via NO release in isolated rat thoracic aorta. *Life Sci*. **2006**, *79*, 1062−1068.
(45) You, H. J.; Choi, C. Y.; Kim, J. Y.; Park, S. J.; Hahm, K. S.; Jeong, H. G. Ursolic acid enhances nitric oxide and tumor necrosis factor-α production via nuclear factor-κB activation in the resting macrophages. *FEBS Lett*. **2001**, *509*, 156−160.

Received for review August 23, 2010. Revised manuscript received October 21, 2010. Accepted October 29, 2010. This work was supported by the National Science Council (NSC 97-2314-B-038-035-MY2, NSC 97-2320-B-039-022-MY3, and 99-2314-B-038-030-MY2), Taiwan.